Auto-Tuning of a Modified L1-Adaptive Controller with Genetic Algorithms for Dynamic Positioning of a Remotely Operated Vehicle Under Marine Currents

Jose Joaquin Sainz[1] * (ID)
Victor Becerra[2] (ID)
Elías Revestido Herrero[1] (ID)
Jose Ramon Llata[1] (ID)
Luciano Alonso-Rentería[1] (ID)

[1] Departamento de Tecnología Electrónica, Ingeniería de Sistemas y Automática, Universidad de Cantabria, Santander, Spain

[2] School of Energy and Electronic Engineering, University of Portsmouth, Portsmouth, United Kingdom

* Corresponding author: sainzjj@unican.es (Jose Joaquin Sainz)

ABSTRACT

In this article, a modified L1-adaptive controller with auto-tuning using a genetic algorithm is presented for dynamic positioning of remotely operated vehicles (ROVs) under marine currents, based on a six-degree-of-freedom nonlinear model of an ROV. To enable tuning of some of the parameters of the controller, a cost function related to the error of the steady state positions of the system is minimised with the use of the genetic algorithm. A series of simulations are conducted to ascertain the performance of the system with the implemented controller, taking into consideration the vehicle position, orientation, and control signals sent as commands to the thrusters. The simulations are carried out with noise levels representative of those encountered by the standard underwater instrumentation on an ROV, as well as with underwater current velocities. In addition, the results are compared with those of a classical controller to verify the improvements offered by the controller proposed in this paper.

Keywords: Auto-tuning; dynamic positioning; genetic algorithm; modified L1-adaptive; ROV

INTRODUCTION

Today, the use of remotely operated vehicles (ROVs) and unmanned underwater vehicles has become widespread, due to their versatility and the multitude of complex and potentially dangerous operations that these vehicles can perform [1]. Zhao [2] described the development of a mathematical and computational model to improve the planning and execution of missions combining different types of marine vehicles such as Autonomous Surface Vehicles (ASVs) and ROVs. In work by Fay [3], the design of ecological interfaces was proposed as

a paradigm for ROVs, to facilitate optimal future performance and the interaction between a human and the ROV interface. Soylu [4] presented a method for the precise control of the trajectory of an ROV for inspection to improve accuracy when performing inspection tasks. These applications are related to exploration and research, the offshore energy industry, underwater archaeology, environmental monitoring, search and rescue operations, infrastructure inspection, defence and security, aquaculture and fisheries, underwater filming, hazardous environment exploration, pipeline maintenance, and cable installation.

In these applications, the deployment of ROVs requires accurate dynamic positioning systems. Consequently, diverse control methodologies have been applied in this field. Classical control techniques such as proportional, integral, and derivative (PID) techniques were among the first approaches to be applied, for example by Fossen [5], [6]. These techniques were initially used due to their good results and their wide real-world applicability. Moreover, PID control is often used as a benchmark for comparison of the performance of more advanced techniques [7]. Robust control is another technique that is prevalent in this field, due to its ability to mitigate the external disturbances and unexpected phenomena that may occur during the course of operation [8]. A further advanced control technique that is often used in the marine environment for the dynamic positioning of different vehicles and structures is the linear quadratic control (LQR) technique, in which a cost function is minimised to obtain appropriate control signals [9]. The L1-adaptive control technique should also be highlighted as a control technique with significant potential in the field. This advanced control technique combines the use of an LQR control with a Kalman filter with an adaptive loop [10], which allows it to quickly compensate for external disturbances, giving this system a faster and more robust response to disturbances than other types of controllers. This methodology has found applications in various fields, including nuclear plant control [11], the dynamic positioning of ROVs [12], and marine structures [13]. Due to the difficulty of manually tuning the parameters of some control techniques and the need to adjust certain controller parameters according to changes in the system conditions, auto-tuning techniques are often used, as described for example by Goheen [14]. The application of genetic algorithms based on the minimisation of a cost function is noteworthy in this area [15], as their implementation enhances the robustness and accuracy of the system response.

In the present work, we present a modified L1-adaptive controller with autotuning capability for the dynamic positioning of a ROV under marine currents. This is an innovative way of combining and applying these control techniques, as this combination of the control techniques presented in this document has not been found in the literature. The proposed controller for the dynamic positioning of ROVs is illustrated in Fig. 1. The controller is composed of a control loop with a linear quadratic optimal controller, a Kalman filter, and an adaptive loop, creating an L1-adaptive set which has been modified with respect to the conventional application of this control approach. This modification consists of the elimination of a transfer function just after the first subtraction operation in the first feedback loop. A tuning system based on genetic algorithms was also developed to adjust one of the controller parameters in the presence of ocean currents.

Fig. 1. Schematic of the system with the proposed controller

Several simulations were performed, and the results obtained with the modified L1-adaptive controller were compared with those achieved with a PID controller. The results show that the proposed controller positions the ROV accurately and with a significantly lower error than the PID controller, achieving this accuracy while using appropriate control signals for its operation. It is demonstrated that better results are obtained when implementing this type of proposed controller compared to the classical PID controller, as it is observed to be more accurate, with higher speed and robustness against disturbances. This improvement in control accuracy represents a potential extension of the areas of operation in which the ROV can be used. In particular, the improved stability and precision of movement will potentially allow for the use of an ROV in underwater inspection tasks, where this level of control performance is required to capture high-quality images.

MATHEMATICAL REPRESENTATION OF THE ROV

To describe the motion of the ROV model Bluerov2 with a heavy configuration with eight thrusters (see Fig. 2), it is necessary to use three rotational coordinates and three translational coordinates.

To study the motion of the ROV, two coordinate systems are considered. The first is fixed to the vehicle (BODY-frame) and determines its translational and rotational motions, while the second is located on the Earth (NED-frame) and describes the position and orientation of the vehicle (see Fig. 2).

Fig. 2. Frames of reference used: BODY and NED frames

The nonlinear manoeuvring model can be expressed in the following form [5] (for more details about the model and the value of the parameters, see von Benzon [16]):

$$M\dot{v} + C(v)v + D(v)v + g(\eta) = \tau \quad \textbf{(1)}$$

$$\dot{\eta} = J(\eta)v \; ; \; y_s = \eta + w_n \quad \textbf{(2)}$$

In the NED frame, the position and Euler angle vectors are given by the expression: $\eta = [x,y,z,\phi,\theta,\psi]^T$, and y_s is the output vector with sensor noise. The linear and angular speeds in the body frame velocities are represented by the vector $v = [u,v,w,p,q,r]^T$, while the forces and moments exerted by the thrusters are represented by the vector $\tau = [X,Y,Z,K,M,N]^T$. The vector w_n represents the measurement noise. The matrix M represents the rigid body and added mass, the vector $C(v)v$ denotes the Coriolis term, the matrix $g(\eta)$ represents the restoring matrix, and the matrix $J(\eta)$ is the rotation matrix. The vector $D(v)v$ represents the hydrodynamic damping forces, which are a combination of linear and nonlinear damping.

In the context of ocean currents, as described in the works of Fossen [5] and von Benzon [16], Eq. (1) can be expressed as follows:

$$M_{RB}\dot{v} + M_A\dot{v}_r + C_{RB}(v)v + C_A(v_r)v_r + D(v_r)v_r + g(\eta) = \tau \quad \textbf{(3)}$$

$$v_r = v - v_c \quad \textbf{(4)}$$

The current velocity in the body-fixed coordinate system is:

$$v_c = [V_{cf1}, 0, 0, 0]^T; \; v_{cf1} = J_1(\eta)^T \times V_{cn} \quad \textbf{(5)}$$

where $V_{cn} = [V_{cun}, V_{cvn}, V_{cwn}, 0,0,0]$ is the current velocity in the NED coordinate system, and $J_1(\eta)$ is the first component of the matrix $J(\eta)$. For more details of the model parameters, thrusters, their layout on the ROV, and the system of distributing forces and moments, see von Benzon [16] and Ng [17].

The attenuators At(s) for x,y,z and for ϕ,θ,ψ are:

$$At_{(x,y,z)}(s) = \frac{0.1}{(0.05s)+0.1}; \qquad At_{(\phi,\theta,\psi)}(s) = \frac{0.1}{(0.4s)+0.1} \quad \textbf{(6)}$$

MODIFIED L1-ADAPTIVE CONTROL

This section describes the innovative application of the modified L1-adaptive control method to implement a dynamic positioning application for the ROV illustrated in Fig. 1.

In order to achieve this, the adaptive control approach described by Cao [10] and Hovakimyan [18] is employed in combination with a LQG controller. The implementation follows a similar structure to the one described by Sainz [13],

in which this system was used for the control of a marine structure, and by Vajpayee [11], where this controller was used for the control of a nuclear power plant.

The state-space linearisation of the nonlinear model of equation Eq. (1) is carried out as follows:

$$\dot{x}_L(t) = A_L \, x_L(t) + B_L[u_r(t)] \quad \textbf{(7)}$$

$$y_L(\text{t}) = C_L x_L(t) + D_L[u_r(t)] \quad \textbf{(8)}$$

where
- $u_r = \tau$ are the forces and moments generated by the thrusters;
- A_L is the state matrix;
- $x_L(t) = [x_L, y_L, z_L, \phi_L, \theta_L, \psi_L]^T$ is the state vector, the elements of which correspond to the position and the Euler angles vector of the linearised model;
- BL is the input matrix;
- CL is the output matrix;
- $y_L(t) = [x_L, y_L, z_L, \phi_L, \theta_L, \psi_L]^T$ is the output vector;
- DL is the feedforward matrix.

The linearised model in Eq. (7) was obtained by linearising the system around the starting conditions of the system. The Kalman filter is also implemented to filter sensor noise from the position signals that are used in the control system, by considering the linear model of the ROV in Eq. (7). The Kalman filter is implemented using an algorithm described in detail by Fossen [19] and more extensively explained in [5]. The algorithm is as follows:

- Matrix design:

$$Q(t) = Q^T > 0; \quad R(t) = R^T > 0; \quad \hat{x}_{f(0)} = x_{f(0)} \quad \textbf{(9)}$$

- Initial conditions:

$$P(0) = E[(x_{f(0)} - \hat{x}_{f(0)})(x_{f(0)} - \hat{x}_{f(0)})] \quad \textbf{(10)}$$

- Kalman propagation matrix:

$$K(t) = P(t)C^T(t)R^{-1}(t) \quad \textbf{(11)}$$

where P is the solution of the algebraic Riccati equation.
- Propagation of estimated states

$$\dot{\hat{x}}_{f(t)} = A_L(\text{t})\hat{x}_{f(t)} + B_L(\text{t})u_r(t) + K(t)[y_f(t) - C(t)\hat{x}_{f(t)}] \quad \textbf{(12)}$$

In this context, the tuning variables are represented by the terms Q and R, which correspond to the covariances of the states and the covariances of the noise, respectively. The term u_r denotes the forces and moments generated by the thrusters, while the term y_f represents the Kalman filter output vector. The estimated state vector is given by the expression $\hat{x}_f$, while the filtered state vector is represented by the equation $\hat{x}_f = y_f$

$$F_c(t) = -u_{LQR}(t) + u_a(t) \quad \textbf{(13)}$$

The term $u_{LQR}(t)$ denotes the nominal control signals of the LQR controller, whereas $u_a(t)$ represents the adaptive control. The linear feedback of the control state is calculated by minimising the cost function

$$u_{LQR} = -K_{LQR}x_f \qquad (14)$$

The cost function was set up as described by Fossen [5]:

$$J(u) = \int_0^\infty [x_f^T Q_{LQR} x_f + u_r^T R_{LQR} u_r] dt \; ; \; K_{LQR} = R_{LQR}^{-1} B_{LQR}^T P_{LQR} \qquad (15)$$

P_{LQR} is calculated by solving the algebraic equation of Riccati:

$$A_L^T P_{LQR} + P_{LQR} A_L - P_{LQR} B_L R_{LQR}^{-1} B_L^T P_{LQR} + Q_{LQR} = 0 \qquad (16)$$

The matrix Q_{LQR} is employed as a tuning parameter, while the matrix R_{LQR} represents the second of the controller tuning parameters for the LQR controller.

The state in Eq. (7) can be expressed as follows:

$$\dot{x}_L(t) = A_m x_L(t) + B_m[\omega_0 u_a(t) + \sigma_1(t)] \qquad (17)$$

The closed loop system matrix, denoted by A_m, can be expressed as follows: $A_m = A_L - B_m K_L^T QR$, where K_{LQR} represents the control feedback gain. The input matrix is represented by $B_m = B_L$. The disturbance is represented by the function $\sigma_1(t)$, and the input gain matrix by the function ω_0. This indicates the cross-coupling between different inputs.

$$\omega_0(t) = \begin{bmatrix} 1 & 0 & 0 \\ 0 & 1 & 0 \\ 0 & 0 & 1 \end{bmatrix} \qquad (18)$$

The control system consists of two distinct components: the first is a linear quadratic Gaussian controller, while the second is an adaptive controller comprising the FF, PE, PA and PB blocks illustrated in Fig. 1.

$$\dot{\hat{x}}_a = A_m(t)\hat{x}_a(t) + B_m[\omega_0 u_a(t) + \hat{\sigma}_1(t)] \qquad (19)$$

In this case, the estimated state vector of the adaptation part, denoted by the variable $\hat{x}a(t)$, represents the estimated state of the system. Similarly, the output vector, represented by $\hat{y}_a(t)$, is the estimated output of the system. The input matrix, $B_m = B$, represents the input to the system. The estimated disturbance $\hat{\sigma}_1(t)$ is a variable that represents the estimated disturbance in the system. Finally, the input gain matrix of the system is ω_0. Once the states have been estimated, a subtraction is performed with the filtered states, resulting in the prediction error, denoted as $\tilde{x}$.

$$\tilde{x} = \hat{x}_a(t) - x_f(t) \qquad (20)$$

The methodology employed for projecting disturbances is in accordance with the procedures delineated by Hovakimyan [18] and by Vajpayee [11] for a process control application in a nuclear power plant, in the work of Sainz [13] for a controller for marine structures, and for ROVs with disturbance rejection [10].

$$\dot{\hat{\sigma}}_1(t) = \Upsilon Proj(\hat{\sigma}(t) - (\tilde{x}^T(t)P_m B_m)^T) \qquad (21)$$

The projection operator Proj is defined as follows [20]. In this context, the notation P_m represents the solution of the algebraic Lyapunov equation, while the parameter θ_{max} is defined as the norm limit, and the tolerance in the projection is represented by the term ε_θ. The adaptation gain, which is denoted by the symbol Υ, is given by the expression in Eq. (21). Once the disturbances have been estimated, a preparatory step is taken to calculate the intermediate variable, which is defined by the expression for $\hat{\eta}(s)$:

$$\hat{\eta}(s) = \omega_0 u_a(s) + \hat{\eta}_1(s) \qquad (22)$$

where $\hat{\eta}_1(s) = \hat{\sigma}_1(s)$.

The structure of the adaptive control law is as follows:

$$u_a(s) = -(\hat{\eta}(s) - r_{ffp}(s)) \qquad (23)$$

where $r_1(s)$ is the reference signal after the attenuator

$$r_1(s) = r(s)At; \qquad r_{ffp}(s) = r_1(s) \times K_g \qquad (24)$$

The quantity represented by K_g corresponds to the value of the feedforward filter, which is also known as a feedforward pre-filter. This filter is configured in such a way that the overall system is provided with the requisite conditions for effective control, with the signals being decoupled.

It should be noted that the usual structure of the L1-adaptive controller has been modified by eliminating the integral action that is usually incorporated between the two loops of the controller. This integral action can be eliminated due to the implementation of an auto-tuning system based on the genetic algorithm to tune the control parameter K_g to obtain the desired response and reducing the stationary state error.

AUTO-TUNING WITH THE GENETIC ALGORITHM

In the proposed method described in the previous section, several tuning parameters need to be properly set to obtain the desired response from the system, due to the complexity of the controller. In addition to the parameters corresponding to the Kalman filter and the LQR controller, there are other parameters specific to the L1-adaptive control. The system response is highly sensitive to the tuning of the K_g parameter, corresponding to the feed-forward prefilter. Hence, an auto-tuning process for the parameter was established using the genetic algorithm [21].

A genetic algorithm is used to tune the K_g with the aim of reducing to a minimum the error in the ROV position output by performing the steps shown in Fig. 3.
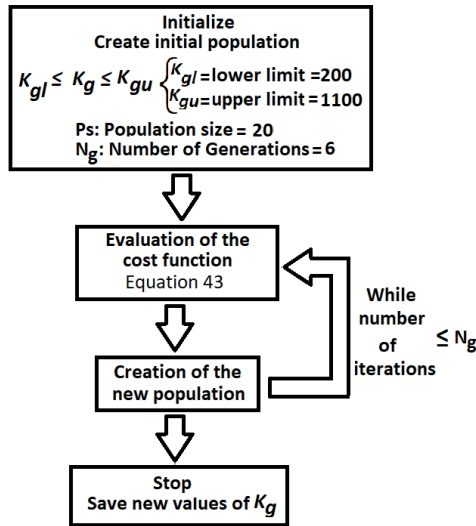
Fig. 3. Genetic algorithm

$$J_{GA} = |r_1(s) - y_f| \times time \qquad (25)$$

where $r_1(s)$ is the reference signal after attenuation, and y_f is the Kalman filter output vector.

SIMULATION RESULTS AND DISCUSSION

A series of simulations were conducted in the MATLAB-Simulink environment to ascertain the viability of the proposed control scheme, using a sampling period of 0.1 s.

In the simulations, the reference vector was set to $r(s) = [1m, 1m, 1m, 0rad, 0rad, 0rad]^T$, and the Kalman filter matrices were adjusted as follows:

- $Q = diag([1,1,1,9,12,30,1,1,1,900,900,900])$
- $R = diag([0.001,0.001,0.0001,10^{-1}, 10^{-1}, 10^{-1}, 10^{-1}, 10^{-1}, 10^{-1}, 10^{-1}, 10^{-1}])$

The LQR tuning matrices were adjusted as follows:

- $Q^{LQG} = diag([1.99 \times 10^3, 0.300 \times 10^3, 0.013 \times 10^3, 0.005 \times 10^3, 0.005 \times 10^3, 0.005 \times 10^3, 0.005 \times 10^3, 0.005 \times 10^3, 0.005 \times 10^3, 0.005 \times 10^3, 0.005 \times 10^3, 0.005 \times 10^3])$
- $R_{LQG} = diag([0.0035, 0.0015, 0.0002, 0.5, 0.5, 0.5, 0.5, 0.5, 0.5, 0.5, 0.5, 0.5])$

Tab. 1. Tuning parameters for the modified L1-adaptive control

Kg	Υ	ε
[965.01, 866.02, 360.33, 1, 1, 1]	[0.1, 15, 12]	[0, 30, 30, 3]

A PID controller was also implemented (Eq. 26) to determine the improvements offered by the proposed controller compared to a classical PID control with the tuning parameters given in Table 2. The references and filter were the same in both scenarios. Consequently, the scenarios in which the simulations were carried out are identical, except that the proposed controller was replaced by the PID controller, as can be seen from Fig. 4.

Tab. 2. Tuning parameters for the PID controller

P	[1356.97,764.73,609.1827,391.93,81.43,4.4466]
I	[80.49, 1.31, 152.28, 293.52, 76.20, 0.6539]
D	[0, 0, 2.08, 12.64, 20.38, 7.41]
N	[0,100, 2.08,100, 136.40, 17.66]

$$PID(s) = P + I\frac{1}{s} + D\frac{I}{1+N\frac{1}{s}} \qquad (26)$$
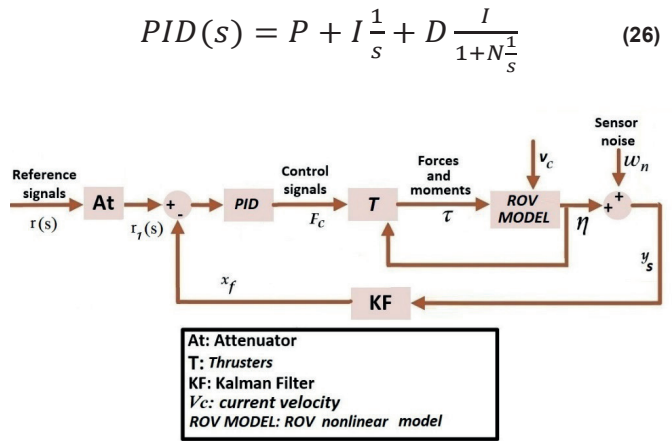
Fig. 4 Schematic of the system with the PID controller

Fig. 5, which represents the motion of the ROV in the x-direction, shows how the controller is able to follow the reference signal without overshoot or oscillations that could lead to a collision with objects or other underwater vehicles. The steady-state error for the implemented controller with self-tuning is approximately 0% of the reference signal. This is acceptable, since it can be observed that the currents that were incorporated into the system are being adequately compensated. Fig. 5 shows that the Kalman filter performs acceptable filtering of the signals.
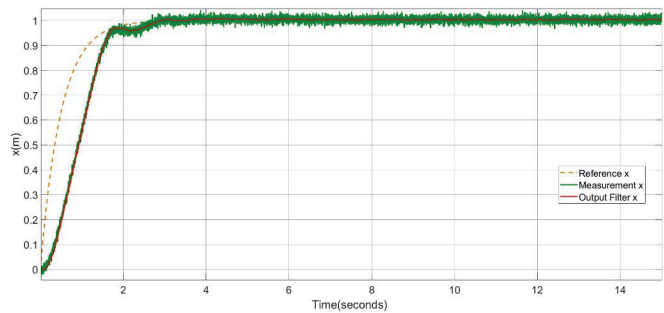
Fig. 5. Results for the ROV with modified L1-adaptive controller for position in the x-direction.

Moreover, it can be observed from Fig. 5 and Fig. 6 that the response at the surge output of x for the modified L1-adaptive controller does not show overshoot or any subsequent attenuation until the response converges to the reference, as in the response for the system with the PID.
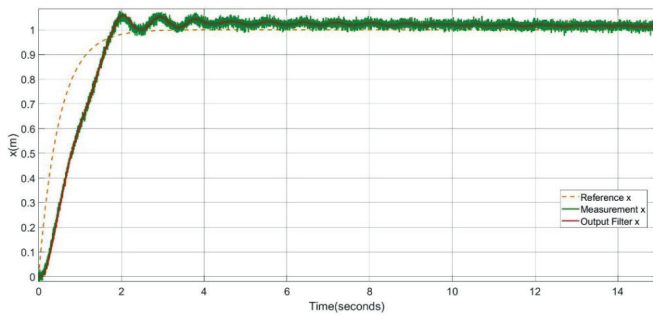
Fig. 6. Results for the ROV with PID controller for position in the x-direction.

Fig. 7 shows the movement along the *x-, y-* and *z*-axes of the system with the PID controller. As in the previous cases, a higher deviation is observed when carrying out the motion to arrive at the reference position than when carrying out the motion with the modified L1-adaptive controller, as shown in Fig. 8.
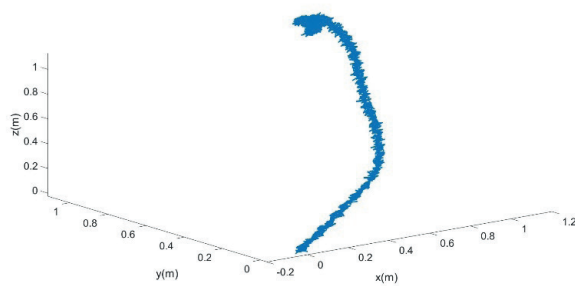

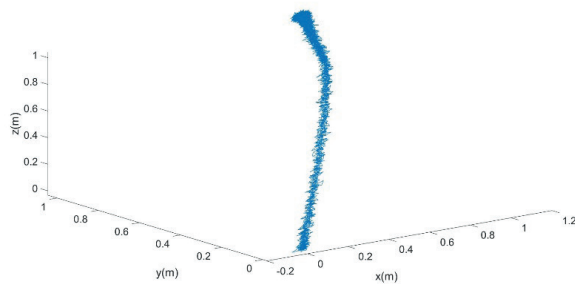Fig. 7. Results for the ROV with PID controller for the positions in the x-, y- and z-directions

Fig. 8. Results for the ROV with modified L1-adaptive controller for the positions in the x-, y- and z-directions

It can be observed from Fig. 9 that the system despite the external perturbations induced by the currents on three of the axes, presents slight steady state errors in roll, pitch, and yaw motions (ϕ, θ, ψ), which can be considered negligible.
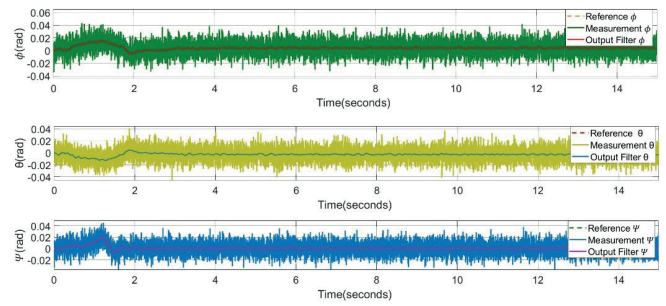
Fig. 9. Results for the ROV with modified L1-adaptive controller for the position in the directions.

The response in terms of the angular movements of both controllers in the steady state is correct, since the deviation in regard to the reference is very small, as can be seen in Fig. 10 for the PID controller and in Fig. 9 for the modified adaptive controller. However, from the output of the PID controller under pitch, it can be seen that during the manoeuvres, the deviation from the reference shown in Fig. 10 is considerably higher than for the modified L1-adaptive controller in Fig. 9.
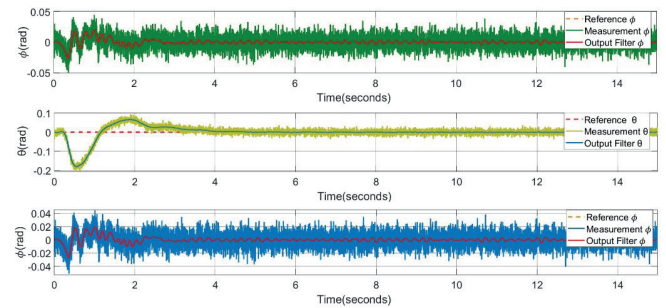
Fig. 10. Results for the ROV with PID controller for positions in the directions.

It can be seen from Fig. 11 that the control signals present no steady-state oscillations and the control effort is low. This leads to an increase in the actuators' service life, and means that an actuation margin can be maintained in the case where marine conditions require it.
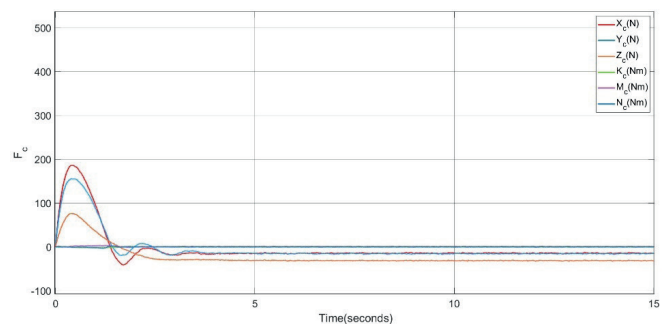
Fig. 11. Results for the ROV with modified L1-adaptive controller for the control signal calculated by the controller

Finally, a comparison of the control signals for the PID controller (Fig. 12) and the proposed modified L1-adaptive controller (Fig. 11) shows that for the PID controller, there is

greater oscillation and higher values of the control signals, which translates into a more demanding performance requirement for the actuators of the system, and hence to a reduction in the life expectancy of the actuators.
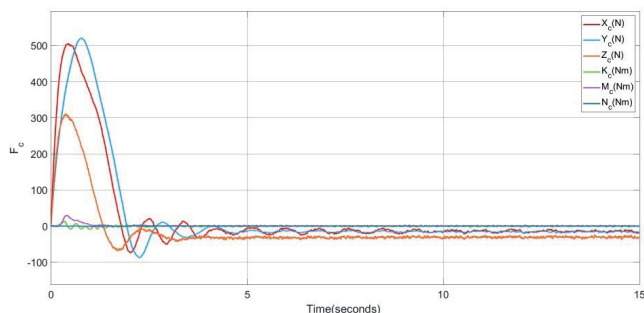

Fig. 12. Results for the ROV with PID controller for the control signal calculated by the controller

As a consequence of the abovementioned effect, the control signals in the thrusters of the system (–1 to 1) also reflect an improvement in the results of the ROV with the modified L1-adaptive controller. It can be observed from Figs. 13 to 16 that the modified L1-adaptive controller only reaches saturation at the beginning of the results for thrusters 2 and 3, and for a shorter time, without other saturation events. From a comparison between the previous results and the results for the ROV with the PID controller, it can observed that the ROV shows saturation of the signals for all the thrusters, over a longer period, with oscillations in the saturation in some cases.
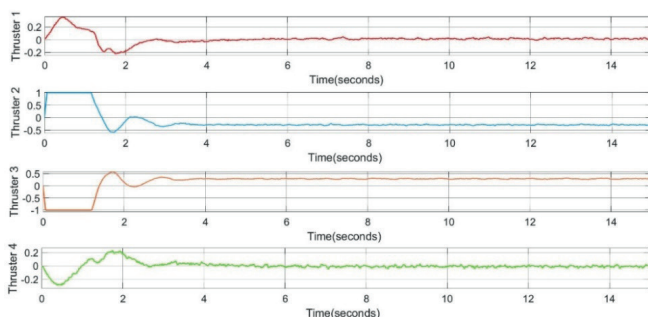
Fig. 13. Results for the ROV with modified L1-adaptive controller for the signals of thrusters 1-4; for more details on the thrusters and their layout on the ROV, see von Benzon [16]
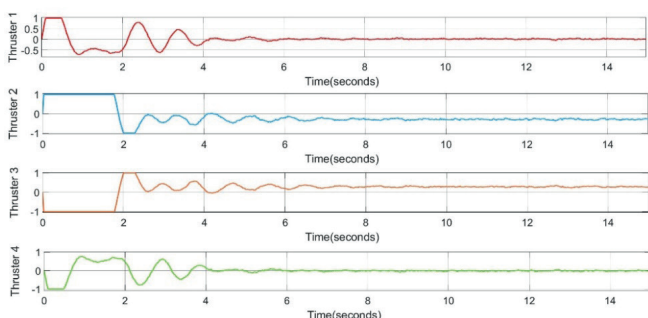
Fig. 14. Results for the ROV with PID controller for the signals of thrusters 1-4
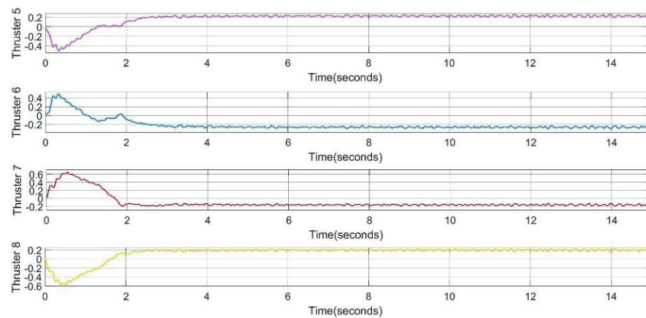
Fig. 15. Results for the ROV with modified L1-adaptive controller for the signals of thrusters 5-8
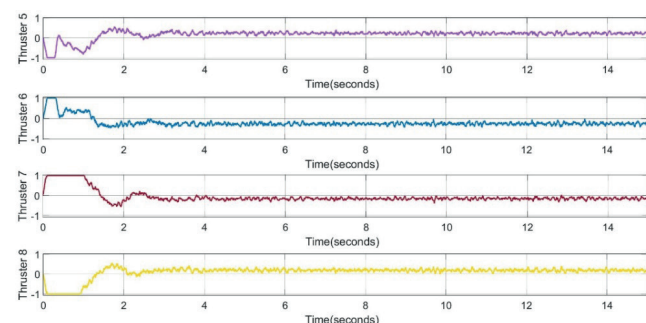

Fig. 16. Results for the ROV with PID controller for the signals for thrusters 5–8

CONCLUSION

In this paper, we have presented a modified L1-adaptive control with autotuning using a genetic algorithm for the dynamic positioning of an ROV subject to undersea currents. Dynamic control is performed in the presence of disturbances corresponding to a standard level of noise for this type of vehicle instrumentation and currents inducing motion along three of the axes. Hence, the dynamic marine environment in which an ROV operates is realistically represented. Several simulations were carried out to verify the correct behaviour of the proposed controller and the autotuning established with the genetic algorithm. Simulation results showed that the implemented controller accurately positioned the ROV at the reference point, and there were no oscillations or overshoots during the positioning manoeuvre. A Kalman filter correctly performed filtering of the ROV positioning signals, and contributed to achieving suitable control signals.

In addition, the control signals were adequate, as they did not exhibit abrupt oscillations; this means that the actuators can have a longer service life, and if the marine environment conditions become worse, the desired position can still be maintained. A comparative study of the proposed controller against a PID controller was also carried out. For all the reasons mentioned in the previous section, it can be concluded that under all the movements studied, the proposed modified L1-adaptive controller produced a better response than the

PID controller. The simulations showed that there was no overshoot and no oscillation.

This system would allow an ROV to operate in scenarios where there is a possibility of collision with other objects, and where precise motion control is required. Similarly, when capturing images using underwater vision instruments, the vehicle is sometimes required to remain as stable as possible. It is notable that with the modified L1-adaptive controller, the oscillations in these positions, which are otherwise present with the classical PID controller, are eliminated. In addition, the control signals of the proposed controller are more desirable than those of the PID controller because they do not undergo such strong oscillations, meaning a greater life expectancy for the actuators. Hence, the proposed controller extends the operational range over which an ROV can operate, due to the possibility of superior control of the vehicle with increased safety for both the human operators and the equipment involved.

The proposed controller also offers a significant advantage for underwater vision, an area which is currently expanding due to the need for supervision of offshore structures and transoceanic pipelines, since if stability can be adequately maintained while the vehicle is moving, it is possible to improve the image capture process and thus simplify the subsequent processing required. Finally, in addition to all the benefits of applying the proposed controller to ROVs that have been highlighted here, which already represent a significant advance, it should be noted that the application of the genetic self-tuning algorithm significantly reduces the difficulty of tuning the controller's parameters. As a result of this self-tuning process, the controller response is robust and adequate, without the need for difficult manual tuning. It may not have been possible to obtain the excellent results presented here with manual tuning.

REFERENCES

1. Amundsen HB, Caharija W, Pettersen KY. Autonomous ROV inspections of aquaculture net pens using DVL. IEEE Journal of Oceanic Engineering 2022, vol. 47, pp. 1-19. https://doi.org/10.1109/JOE.2021.3105285.

2. Zhao C, Thies PR, Johanning L. Offshore inspection mission modelling for an ASV/ROV system. Ocean Engineering 2022, vol. 259, p. 111899. https://doi.org/10.1016/j.oceaneng.2022.111899.

3. Fay D, Stanton N, Roberts APJ. Exploring ecological interface design for future ROV capabilities in maritime command and control. In: Stanton, N. (ed.) Advances in Human Aspects of Transportation. AHFE 2018. Advances in Intelligent Systems and Computing, vol. 786. Springer, Cham. http://dx.doi.org/10.1007/978-3-319-93885-1_24.

4. Soylu S, Proctor AA, Podhorodeski RP, Bradley C, Buckham BJ. Precise trajectory control for an inspection class ROV. Ocean Engineering 2016 vol. 111, pp. 508-523. https://doi.org/10.1016/j.oceaneng.2015.08.061.

5. Fossen TI. Handbook of marine craft hydrodynamics and motion control. John Wiley and Sons, Ltd; 2011. https://doi.org/10.1002/9781119994138.

6. Fossen TI. Marine control systems: Guidance, navigation and control of ships, rigs and underwater vehicles. Marine Cybernetics; 2002.

7. Cao Y, Li B, Li Q, Stokes AA, Ingram DM, Kiprakis A. A nonlinear model predictive controller for remotely operated underwater vehicles with disturbance rejection. IEEE Access 2020, vol. 8, pp. 158622-158634. https://doi.org/10.1109/ACCESS.2020.3020530.

8. Zheng H, Wu J, Wu W, Zhang Y. Robust dynamic positioning of autonomous surface vessels with tube-based model predictive control. Ocean Engineering 2020, vol. 199, p. 106820. https://doi.org/10.1016/j.oceaneng.2019.106820.

9. Sainz JJ, Revestido Herrero E, Llata JR, Gonzalez-Sarabia E, Velasco FJ, Rodriguez-Luis A, Fernandez-Ruano S, Guanche R. LQG control for dynamic positioning of floating caissons based on the Kalman filter. Sensors 2021, vol. 21. pp. 1-18. https://doi.org/10.3390/s21196496

10. Cao C, Hovakimyan N. L1 adaptive controller for systems with unknown time-varying parameters and disturbances in the presence of non-zero trajectory initialization error. International Journal of Control 2008, vol. 81, pp. 1147-1161. https://doi.org/10.1080/00207170701670939

11. Vajpayee V, Becerra V, Bausch N, Deng J, Shimjith SR, Arul AJ. L1-adaptive robust control design for a pressurized water-type nuclear power plant. IEEE Transactions on Nuclear Science 2021, vol. 68, pp. 1381-1398. https://doi.org/10.1109/TNS.2021.3090526

12. Maalouf D, Creuze V, Chemori A. A novel application of multivariable L1 adaptive control: From design to real-time implementation on an underwater vehicle.

Proceedings of the IEEE International Conference on Intelligent Robots and Systems (IROS), 7-12 October 2012. Vilamoura-Algarve, Portugal. DOI: https://doi.org/10.1109/IROS.2012.6385498.

13. Sainz JJ, Becerra V, Revestido Herrero E, Llata JR and Velasco FJ. L1 adaptive control for marine structures. Mathematics (Basel) 2023, vol. 11, p. 3554. https://doi.org/10.3390/math11163554

14. Goheen KR, Jefferys ER. Multivariable self-tuning autopilots for autonomous and remotely operated underwater vehicles. IEEE Journal of Oceanic Engineering 1990, vol. 15, pp. 144-151. https://doi.org/10.1109/48.107142

15. Tanveer A, Ahmad SM. High fidelity modelling and GA optimized control of yaw dynamics of a custom built remotely operated unmanned underwater vehicle. Ocean Engineering 2022, vol. 266, p. 112836. https://doi.org/10.1016/j.oceaneng.2022.112836

16. Von Benzon M, Sørensen FF, Uth E, Jouffroy J, Liniger J, Pedersen S. An open-source benchmark simulator: Control of a BlueROV2 underwater robot. Journal of Marine Science and Engineering 2022, vol. 10, p. 1898. https://doi.org/10.3390/jmse10121898

17. Ng P, Krieg M. Modifications to ArduSub that improve BlueROV SITL accuracy and design of hybrid autopilot. Applied Sciences 2024, vol. 14, no. 17, p. 7453. https://doi.org/10.3390/app14177453

18. Hovakimyan N, Cao C. L1 adaptive control theory: Guaranteed robustness with fast adaptation. Society for Industrial and Applied Mathematics 2010. https://doi.org/10.1137/1.9780898719376

19. Fossen TI, Perez T. Kalman filtering for positioning and heading control of ships and offshore rigs. IEEE Control Systems Magazine 2009, vol. 29, pp. 32-46. https://doi.org/10.1109/MCS.2009.934408

20. Pomet J, Praly L. Adaptive nonlinear regulation: Estimation from the Lyapunov equation. IEEE Transactions on Automatic Control 1992, vol. 37, pp. 729-740. https://doi.org/10.1109/9.256328

21. Goldberg DE. Genetic algorithms in search, optimization, and machine learning. Addison-Wesley; 1989.